Journal of Electroanalytical Chemistry 807 (2017) 228–234

Contents lists available at ScienceDirect

Journal of Electroanalytical Chemistry

journal homepage: www.elsevier.com/locate/jelechem

Understanding the mechanism of TiO_2 nanotubes formation at low potentials (≤ 8 V) through electrochemical methods

U.H. Shah[a], K.M. Deen[b], H. Asgar[a], Z. Rahman[c], W. Haider[a,c,*]

[a] School of Engineering and Technology, Central Michigan University, Mt. Pleasant, MI, USA
[b] Department of Materials Engineering, University of British Columbia, Vancouver, BC V6T 1Z4, Canada
[c] Science of Advanced Materials, Central Michigan University, Mt. Pleasant, MI, USA

ARTICLE INFO

Keywords:
Titanium dioxide nanotubes
Lewis species
Spectroscopy
Electrochemsitry

ABSTRACT

The electrochemical characterization of cpTi–2 during anodization was carried out to understand the formation of nano–tubular structure at different applied potentials (≤ 8 V). The linear sweep voltammetry, potentiostatic polarization and impedance spectra analyses were conducted to estimate the possible reaction sequence during anodization in fluoride and phosphate containing electrolyte. Effect of applied potential on the surface morphology was examined under scanning electron microscope. The generation of Lewis acid active sites within the pre-formed passive film beyond the critical potential (≥ 1.9 V vs. SCE) would enhance the growth of oxide film with simultaneous localized dissolution by the formation of $[TiF_6]^{2-}$ complex. It has been evaluated that the competitive field assisted oxidation and field enhanced dissolution processes at the surface would result in the formation of nano–tubular morphology at the surface of Ti.

1. Introduction

Titanium dioxide nano-tubular structure has very attractive electrochemical characteristics due to its wide band gap, electrical conductivity and chemical stability in very aggressive environments. Owing to these properties, this material has been studied vigorously in the past for many applications i.e. for photo-catalysis, water splitting, dye degradation and for bio-implants [1–3]. The nanotubes have been grown on Ti substrate by, hydrothermal, template assisted growth, electrochemical anodization and sol-gel methods. The electrochemical anodization is the simplest and more organized approach to form titanium dioxide nano-tubes (TNTs) on Ti or its alloys [4]. The morphology of TNTs can be simply tuned by adjusting the process parameters i.e. potential, pH, anodization time, solution concentration and by the addition of some specific species in the electrolyte. The electrochemical anodization is a complex process and involves simultaneous but competing field assisted growth and chemical dissolution processes. The formation of titanium dioxide (TiO_2) nano-structure on the Ti and/or its alloys has been widely discussed in the literature [5,6]. The nature and concentration of ionic and non-ionic species (organic) in the electrolyte are the main contributing factors for effective growth and formation of nanotubes [7,8]. It is important to understand the effect of applied potential as same material exhibit different properties as they possess different microstructures with the variation in the applied field.

The effect of applied potential on the anodization of Ti has been discussed in this work. Based on the information obtained from the current transient profile, the influence of overpotential on the surface morphology was investigated. The impedance spectra at high over-potential were obtained to simulate, the in-situ electrochemical processes at the surface during formation and growth of TNTs. The surface features were observed by using scanning electron microscopy (SEM) images to support the electrochemical findings.

2. Materials and experimental setup

2.1. Materials

Commercially pure titanium grade 2 (cpTi-2) (C 0.08%, N 0.03%, O_2 0.25%, Fe 0.2%, H 0.01%, others 0.4% & balance Ti) purchased from Source One Metals® was used to study the TNTs formation mechanism. The analytical grade chemicals i.e. ethylene glycol ($C_2H_6O_2$), ammonium di-hydrogen phosphate ($NH_4H_2PO_4$), ammonium fluoride (NH_4F), glycerol ($C_3H_8O_3$), sodium chloride (NaCl), acetone (CH_3COCH_3), and ethanol (C_2H_5OH), were purchased from Fischer Scientific and used as received without further purification.

* Corresponding author at: School of Engineering and Technology, Central Michigan University, Mt. Pleasant, MI, USA.
E-mail address: haide1w@cmich.edu (W. Haider).

https://doi.org/10.1016/j.jelechem.2017.11.014
Received 18 September 2017; Received in revised form 5 November 2017; Accepted 6 November 2017
Available online 08 November 2017

2.2. Sample preparation

Circular rods (ϕ = 1.6 cm) were cut into thin discs having thickness 0.8 cm using high speed precision cutter. These circular discs were polished sequentially over silicon carbide SiC papers from 180 to 1200 grit size. Further, these disc samples were degreased in acetone, ethanol and deionized water successively by ultra-sonication followed by drying in the nitrogen stream.

2.3. Electrochemical investigation for TNTs formation at low potential (≤ 8 V)

To investigate the formation and growth of TNTs, the linear sweep voltammetry (LSV) and potentiostatic polarization (PSP) tests were conducted in a three-electrode cell connected with Gamry Reference 3000 potentiostat. The graphite rod and saturated calomel electrode (SCE) (240 mV vs. SHE) were used as counter and reference electrodes, respectively. The cpTi-2 disk samples were the working electrodes in this cell setup. The electrochemical tests were conducted at room temperature under steady state conditions in stagnant electrolyte. Prior to each test, the initial delay was applied to achieve stabilized open circuit potential (OCP) with a tolerance of (0.1 mV/min). In order, to ensure the reproducibility, each test was repeated in triplicate. The electrolyte used in this study was composed of ethylene glycol (92 mL), glycerol (0.5 mL), ammonium dihydrogen phosphate (0.1 M), ammonium fluoride (0.3 M) and deionized water (8 mL) as described elsewhere [7]. The LSV scan was obtained by polarizing the sample from OCP to 10 V at a sweep rate of 20 mV/s in the anodizing solution. Based on the current response under dynamic potential variation (LSV trend), the potentiostatic polarization (PSP) tests were also conducted at various potentials to investigate the surface morphology in relation with the electrochemical behavior. The electrochemical impedance spectra (EIS) were also obtained at various DC potentials (under potentiostatic control). The 5 mV AC perturbation was exerted over each applied DC potential under varying frequency from 100 kHz to 10 mHz. The applied DC potential was maintained constant for an hour prior to impedance spectroscopy test.

3. Results and discussions

3.1. Effect of overpotential (≤ 8 V) on the formation of TNTs

Fig. 1a shows the LSV of cpTi-2 in the anodizing solution. The scan was initiated in the positive (anodic) direction with respect to OCP at a sweep rate of 20 mV/s.

The transient in the current response can be divided into three distinct regions. The high current (0.35 mA/cm^2) was observed in region–I, which decreased rapidly to 0.20 mA/cm^2 and remained almost constant up to 1 V. This behavior was associated with the kinetically controlled oxidation of Ti to Ti^{2+} (at relatively small potential near OCP) followed by the formation of thin oxide film with increase in the potential (region–I). Initially, the large current response was related with the oxidation of Ti (reactions (1) and (2)) and would result in the increase of Lewis acid sites at the surface [9]. This could promote the adsorption of OH^- ions from the water molecules which is termed as hydrolysis reaction (reaction (3)). This reaction would appreciably lower the pH at the metal electrolyte interface. The decay in current density corresponded to the formation of hydrated oxide film and suggests the maximum capacity for the water adsorption at the surface of the metal. Further, increase in the potential (region–II) could promote the oxidation of the adsorbed water molecules at the surface leading to the generation of more Lewis acid sites (increasing the holes concentration within the space charge region) at the oxide film. An increase in current density and appearance of prominent current peak at 1.9 V (vs. SCE) was also observed indicating the oxidation of chemisorbed water molecules and formation of $TiO2^{2+}$ at the oxide/electrolyte (O/E) interface according to reaction (4). The increase in the concentration of acceptor sites ($TiO_2{}^{2+}$ species within the thin oxide film) at the (O/E) interface and local decrease in pH (by the generation of H^+ ions) according to reactions (3) and (4) would accelerate the migration of F^- ions towards the surface. In other words, during anodic polarization, the development of strong electric field across the oxide film would enhance the concentration of electron acceptor sites (Lewis acid sites) within the oxide film. Therefore, with increase in potential, the current response beyond this current peak (at 1.9 V; termed as critical potential) would depend on the migration of anions (F^-) and cations (Ti^{4+}) towards the metal/oxide film (M/O) and oxide film/electrolyte (O/E) interface, respectively. The current density in region–III confirmed to these diffusion controlled processes occurring in the opposite direction [7]. The migration of F^- ions towards the O/E interface strongly depends on the concentration in the electrolyte, field strength, pH drop at the surface and concentration of Lewis acid sites within the pre–formed oxide film. It is therefore, evaluated that the competition between field assisted oxidation processes (reactions (1)–(4)) at the M/O interface and field enhanced dissolution due to migration of F^- ions towards the O/E interface (reactions (5) and (6)) would control the formation of nanotubes over Ti substrate [10]. The control of pH of the electrolyte especially at the metal surface is very crucial for uniform growth of one dimensional nano-tubular structure. These reactions suggest that under applied electric field, the uniform

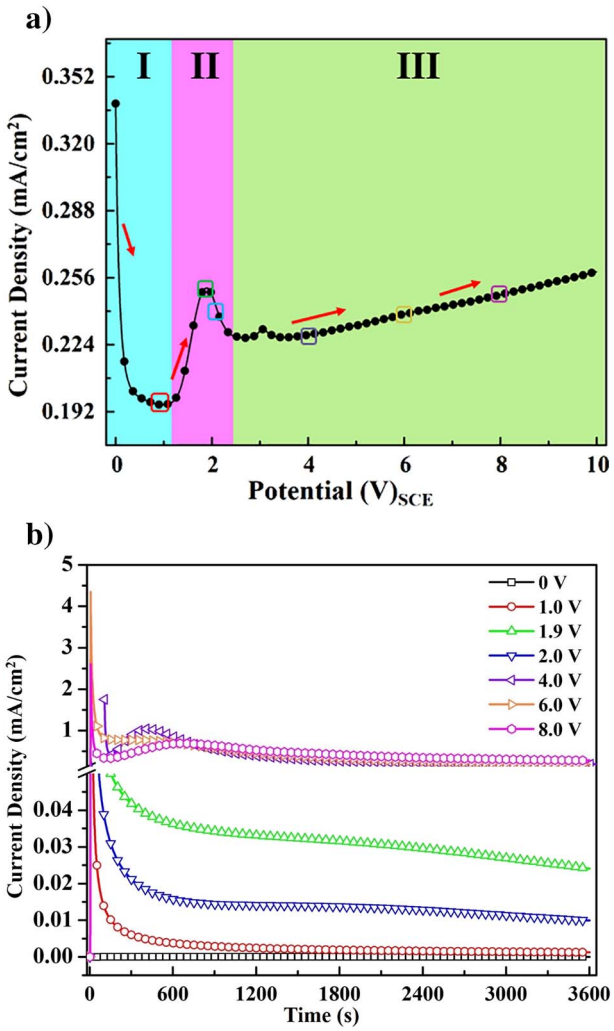

Fig. 1. (a) The LSV trend of cpTi–2 sample at 20 mV/s showing the current potential behavior in the anodizing electrolyte (b) The PSP trends showing the current response at OCP, 1, 1.9, 2, 4, 6 and 8 V (vs. SCE) constant potentials.

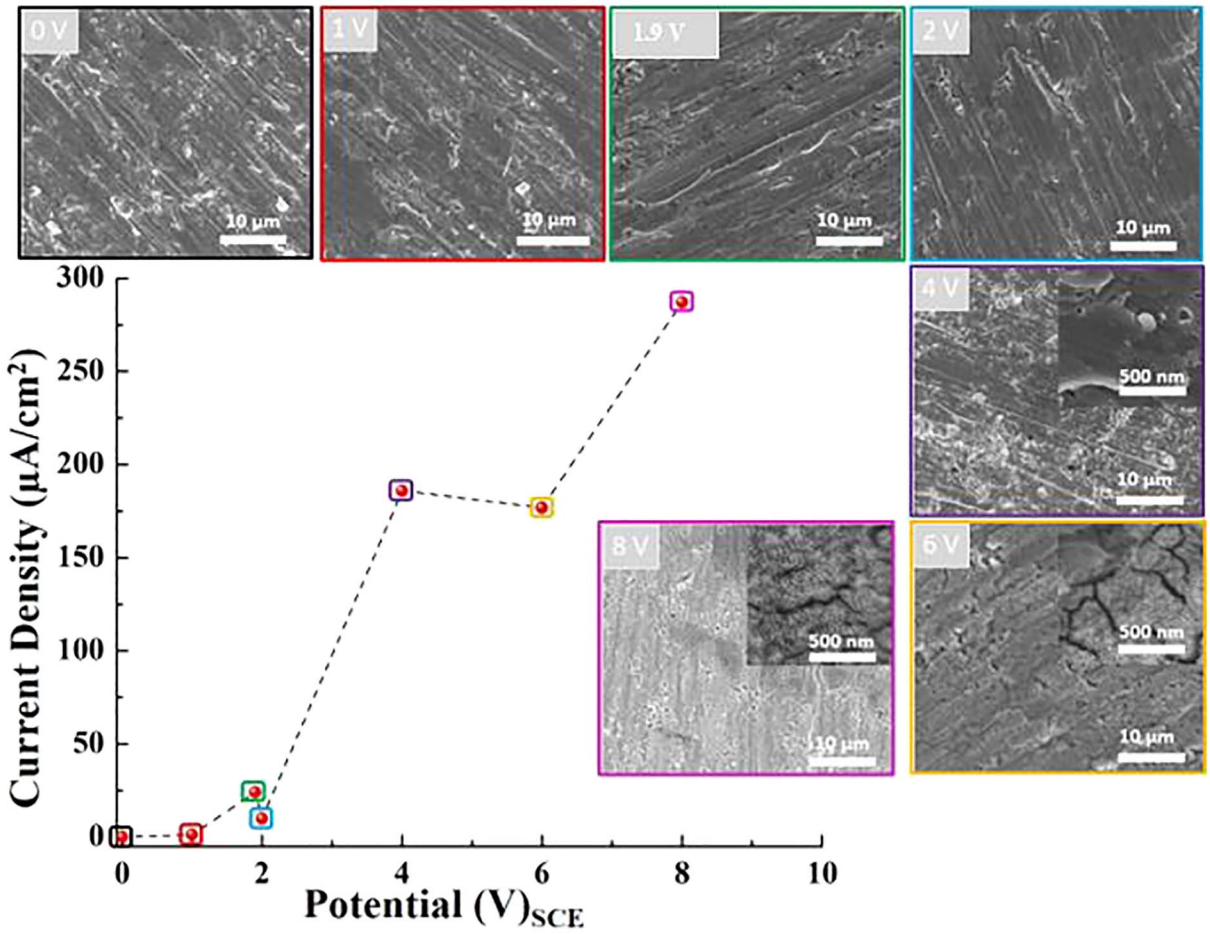

Fig. 2. The trend showing the current values obtained from PSP scans after 1 h polarization. The SEM images depicting the surface morphologies of cpTi–2 samples achieved after 1 h polarization at constant potentials.

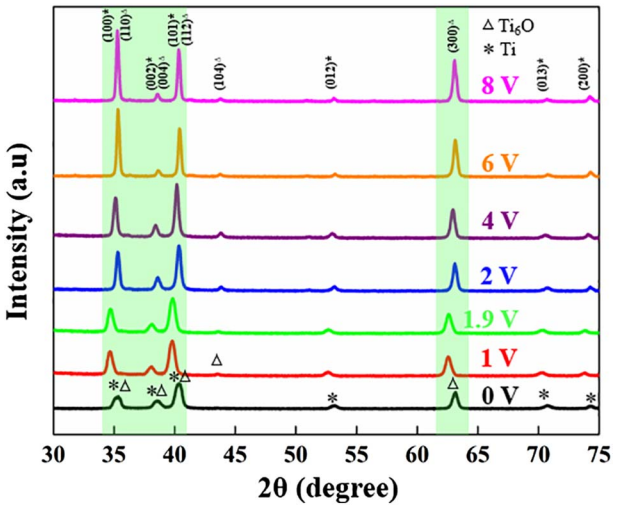

Fig. 3. XRD patterns of cpTi-2 anodized at various potentials. Note: The highlighted area shows the shifting of peak positions.

growth of oxide nanotubes (oxidation processes) would decrease the pH at the M/O interface and dissolution process (reaction (6)) may increase the pH locally within the nano-tube (O/E interface). It is therefore, $NH_4H_2PO_4$ was added in the electrolyte as pH buffering species (reaction (7)) to ensure the uniform growth of nano–tubular structure.

$$Ti \rightarrow Ti^{2+} + 2e^- \quad (1)$$

$$Ti^{2+} \rightarrow Ti^{4+} + 2e^- \quad (2)$$

$$Ti^{4+} + 4H_2O \rightarrow Ti(OH)_4 + 4H^+ \quad (3)$$

$$Ti(OH)_4 \rightarrow TiO_2{}^{2+} + O_2 + 4H^+ + 6e^- \quad (4)$$

$$TiO_2{}^{2+} + 2F^- \rightarrow TiO_2{\cdot}2F_{ads} \quad (5)$$

$$TiO_2 + 6F^- + 4H^+ \rightarrow [TiF_6]^{2-} + 2H_2O \quad (6)$$

$$NH_4H_2PO_4 \leftrightarrow NH_4{}^+ + H_2PO_4{}^- \quad (7)$$

To further explore the formation and growth of nanotubes, the cpTi–02 samples were polarized at constant potentials (PSP scans) for 1 h. The current response at various potentials i.e. 1, 1.9, 2, 4, 6 and 8 V (vs. SCE) is shown in Fig. 1b. The steady state current obtained at each potential after 1 h polarization was measured and plotted as shown in Fig. 2.

The surface morphology of these polarized samples was also examined in the SEM as shown in the inset. At, 1 V the surface of the sample was almost like the one exposed to the same electrolyte for 1 h but at open circuit potential (write value for OCP). The very small current at 1 V was in confirmation with the LSV result (region I) and corresponded to the formation of thin oxide film. The sample polarized at 1.9 V (at the same potential where current peak was observed in the LSV scan) resulted in relatively high current density (24.08 µA/cm^2) which was most likely associated with the oxidation of the thin hydrated layer (reaction (4)) resulting in the development of Lewis acid active sites within the oxide film. The current density again decreased to (9.92 µA/cm^2) at 2 V in support with the LSV scan. This behavior was attributed to the increase in the concentration of the active sites within

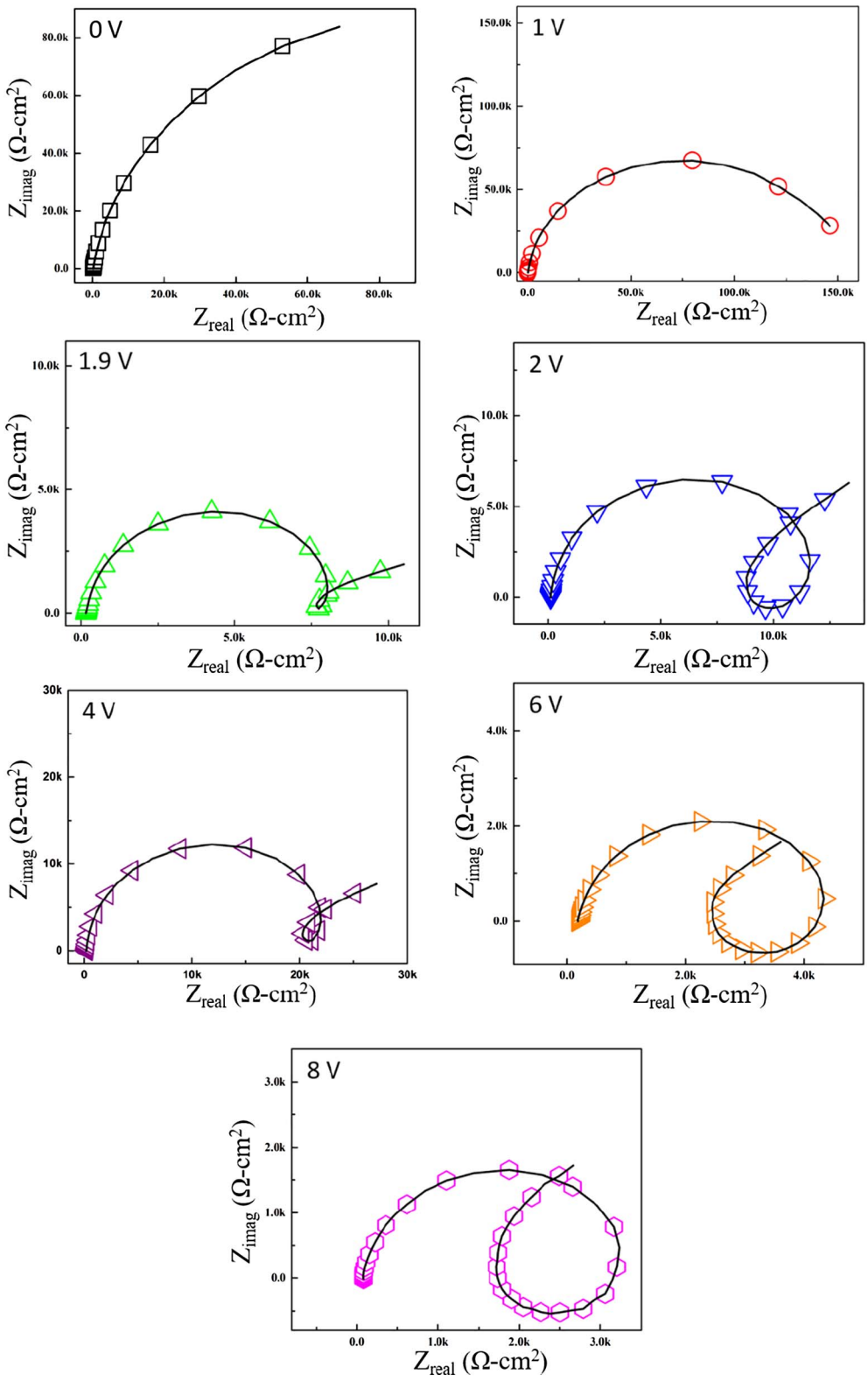

Fig. 4. The impedance spectra data points and fitted curves of cpTi–2 samples at OCP and various applied potentials (≤ 8 V) in the anodizing solution.

the oxide film. The current density increased monotonically beyond 4 V as shown in Fig. 2 corresponding to the field enhanced migration of F^- species towards the active sites (TiO_2^{2+}) and formation of soluble TiF_6^{2-} species. It has been observed that at relative high potential (≥ 4 V) the surface contained some localize pores which at high magnification revealed the formation of nano–tubular structure as shown in the inset of SEM images. It was indicated that with increase in potential (in region III), the competitive field assisted growth and dissolution (formation of $[TiF_6]^{2-}$ species) proceeded simultaneously and resulted in the highly dense nano-tubular structure [11]. It was evaluated that with increase in the potential beyond a critical limit (here reported as 1.9 V) would result in the formation of nanotubes most likely due to the development of Lewis acid active sites and field enhances dissolution (migration and complexation by the F^- ions) processes as discussed

Table 1
Electrochemical parameters obtained after simulating the EEC model with the experimental impedance spectra.

	R_s Ω-cm^2	Y_{dl} μS·s^{n1}·cm^{-2}	n_1	R_p kΩ-cm^2	Y_{ox} μS·s^{n1}·cm^{-2}	n_2	R_{ox} kΩ-cm^2	L H·cm^2	Y_{ads} μS·s^{n1}·cm^{-2}	n_3	R_{dis} kΩ-cm^2	W mS·s$^{0.5}$·cm^{-2}	Fitting goodness
0 V	207.0	90.8	0.91	241.3	–	–	–	–	–	–	–	–	0.7×10^{-3}
1 V	169.1	20.8	0.94	170.5	–	–	–	–	–	–	–	–	0.9×10^{-3}
1.9 V	175.7	10.5	0.96	7.76	0.016	0.96	2.02	805.8	–	–	–	–	1.1×10^{-3}
2 V	126.7	8.0	0.96	1.11	0.0023	0.94	6.66	1907.0	6.27	0.99	7.79	0.445	1.0×10^{-3}
4 V	199.9	6.73	0.99	18.8	0.0058	0.50	7.43	5998.8	394.6	0.98	63.38	0.058	0.3×10^{-3}
6 V	205.7	1.78	0.97	2.558	0.972	0.98	2.24	312.1	387.0	0.98	68.86	1.12	1.2×10^{-3}
8 V	87.29	1.53	0.96	1.87	0.0025	0.45	1.81	129.4	437.7	0.98	2.5	1.51	1.5×10^{-3}

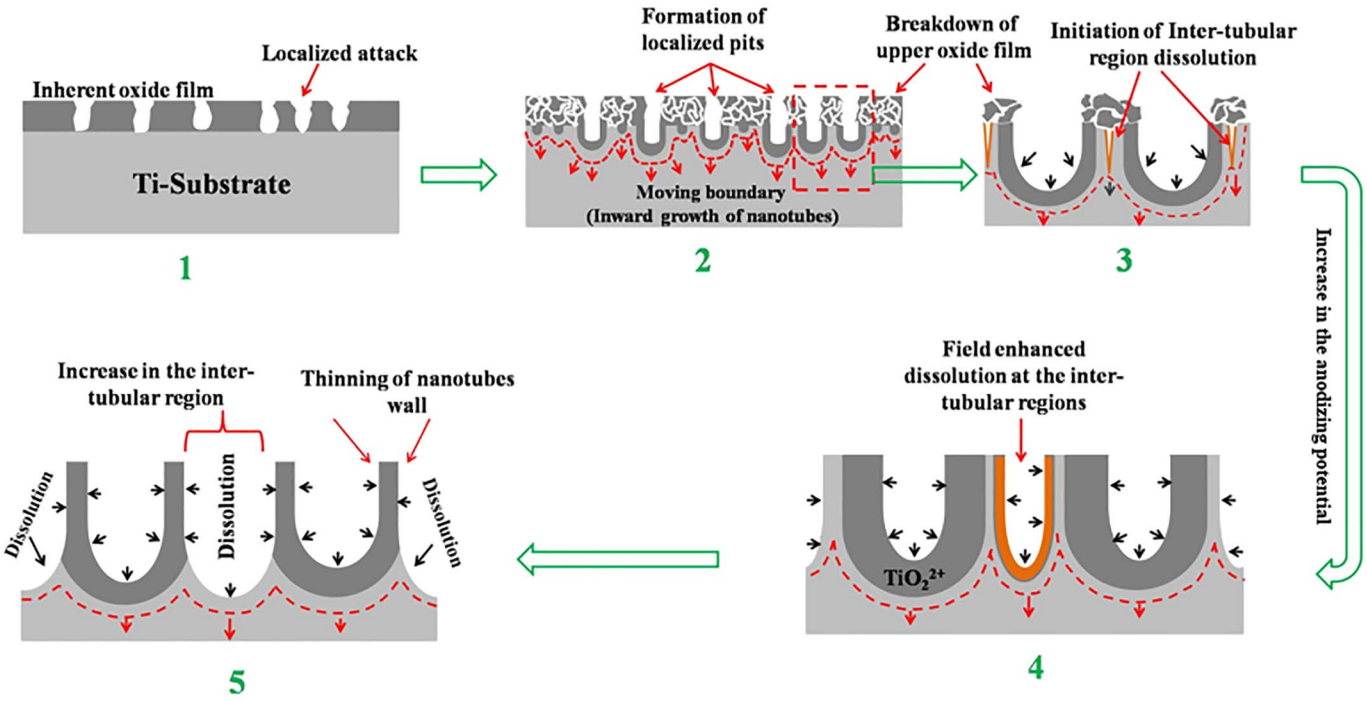

Fig. 5. Schematic representation of nanotubular growth as a function of the applied potential.

above. Fig. 3 shows the XRD patterns of cpTi–2 anodized at various potentials. The XRD patterns matched with the reference patterns COD # 95-152-9956 and COD # 96-900-8518 which corresponded to the Ti_6O (space group *P*-31*c*) and α–Ti (space group *P*63/*mmc*) phases, respectively as given in crystallography open database. It was observed that the diffraction peaks at 2θ = 34.93°, 40.01° and 62.68° depicted the formation of Ti_6O phase and the peaks intensity were found to be directly related with the anodizing potential. At potential < 1.9 V these peaks also shifted to the lower angle which could possibly be either related with the lattice strain (development of compressive stresses) or any change in composition of the surface film i.e. formation of Lewis acid sites. In other words, the shift in diffraction peaks at low potentials and increase in peaks intensity beyond 1.9 V, evidently confirmed the formation and growth of oxygen deficient (Ti_6O) TNTs which also supported our proposed reaction sequence.

The impedance spectra (EIS) obtained at OCP and at various potentials (1, 1.9, 2, 4, 6 and 8 V) are shown in Fig. 4. The equivalent electrical circuit (EEC) models were developed (Fig. 6) to fit the experimental spectra and to simulate the interfacial electrochemical processes occurring at the metal/electrolyte under applied potentials. The quantitative information about the electrochemical parameters used in the EEC models is also provided in Table 1. At OCP and 1 V, the impedance spectra presented one time constant and EEC model is shown in Fig. 6a. The decrease in the solution resistance (R_s) from 207 Ω–cm^2 (at 0 V vs. OCP) to 126.7 Ω–cm^2 (at 2 V) was corresponded to the increase in anions mobility towards the surface under applied electric field. However, the regain of R_s values at 4 and 6 V indicated the balance in the migration of F^- species towards the active sites (TiO_2^{2+}) and formation of soluble TiF_6^{2-} species at the surface. The large applied potential (8 V), the lowest R_s value (87.3 Ω–cm^2) was associated with the surface morphology and could be related with the enhanced ionic activity within the nano–porous structure. The relatively large 'R_p' (241.3 kΩ-cm^2) at OCP compared to 170.5 kΩ–cm^2 obtained at 1 V corresponded to the presence of pre–existing thin passive film which may restrict the charge transfer. However, at 1 V the lower R_p and decrease in the double layer capacitance (presented as constant phase element) (Y_{dl}); 20.8 μS–s^{n1}/cm^2 compared to 90.8 μS–s^{n1}/cm^2 represented the non–uniform distribution of the active sites within the film. Relative to the R_p values observed at low and high applied potentials, the larger R_p (18.8 kΩ-cm^2) at 4 V was also attributed to the limited charge transport across the double layer due to balance in the concentration of active sites (within the surface film) and anionic species at the interface. At critical potential value (1.9 V), the Nyquist plot showed a second time constant as small negative impedance loop followed by increase in the $-Z_{img}$ value at low frequency. This behavior justifies to the development of Lewis acid active site within the oxide film which may enhance the migration of cationic and anionic species (i.e. Ti^{4+} and F^- etc.) towards the O/E and O/M interfaces. This was presented as capacitive (Y_{ox}) and faradaic (R_{ox}) elements in the EEC model. Also, the formation of active sites within the

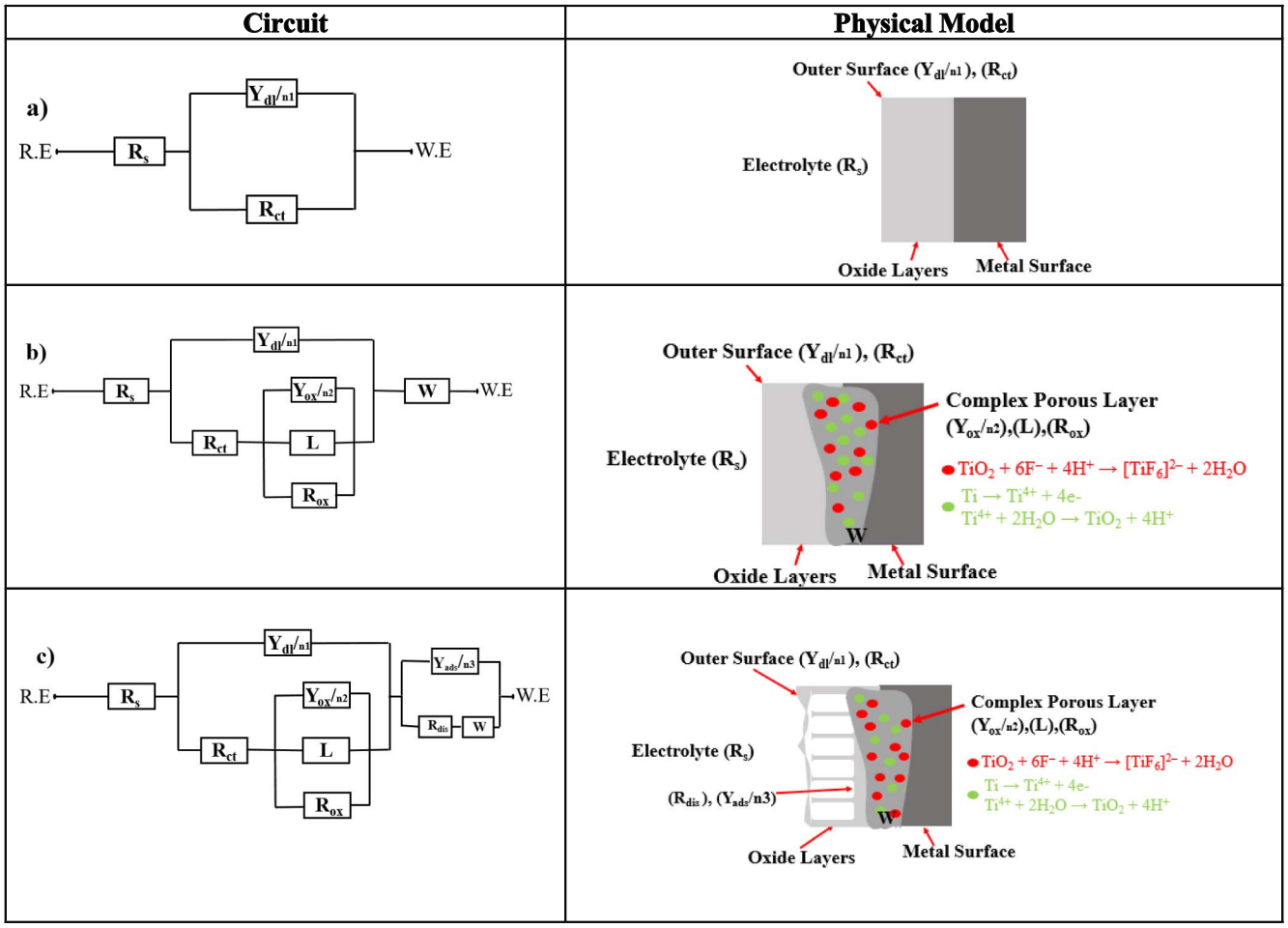

Fig. 6. Equivalent electrical circuit models used to simulate the impedance spectra with the interfacial electrochemical processes for (a) 0 V, 1 V (b) 1.9 V (c) 2, 4, 6 and 8 V.

oxide film could be represented by an inductor (L) as shown in Fig. 6b. Beyond the critical potential (up to 4 V) the slight increase in the Y_{ox} and R_{ox} was affiliated with the charge relaxation and formation of active sites within the oxide film. The large value of 'L' at 2 and 4 V also validated this feature. Further increase in the potential ($\geq$ 4 V) depicted relatively larger loop within low frequency regime attributing to the simultaneous growth and localized dissolution processes, resulted in the formation of nano–tubular structure at the surface [12,13]. The decrease in R_{ox} at high potentials (> 4 V) was also in support with the explanation provided above for reactions (5) and (6). In other words, the high field strength across the oxide film would accelerate the adsorption of F^- species and localized dissolution (due to the formation of soluble complexes; TiF_6^{2-}) would form the nano–porous structure within the oxide film as shown in Fig. 2. This behavior could be simulated with the third time constant as shown in Fig. 6c. The Warburg admittance (W) indicated the migration of ionic species within the electrolyte and across the oxide film.

By considering the electrochemical response of cpTi-2 at low voltages and morphological features observed at various potentials, the mechanism of TNTs formation and growth pattern could be explained. The schematic of TNTs formation and growth pattern is shown in Fig. 5. It is assumed that at the very early stage of nanotubes formation the relatively higher electric field across the inherent TiO_2 oxide film could accelerates the localized dissolution by the action of anionic species in the electrolyte (stage 1). It can be evaluated that penetration of ionic species through the O/E could accelerate local attack at the M/O interface. The presence of small amount of water and anionic species under high applied electric field could enhance the growth of electron deficient TiO_2^{2+} containing oxide film through oxidation at the interface. Simultaneously, the localized dissolution of this defective film is promoted in an organized manner by the anionic species, particularly F^- ions to oxidize at relatively less conductive (TiO_2/TiO_2^{2+}) surface. This occurs by the formation of very small pits underneath the upper oxide film and inward growth of the nanotubes as represented by moving the boundary (stage 2). The combined influence of F^- and H_2PO^{4-} species in the electrolyte and high electric field could modify the growth pattern of TNTs as a function of anodizing potential as discussed above. The field enhanced dissolution and growth will take place simultaneously and this behavior could be verified by the existence of oxide film at the top of nanotubes as evident in Fig. 2. Due to further increase in the anodizing potential, the preferential dissolution at the inter-tubular region and inward growth of the nanotubes would take place simultaneously (stage 3). The dissolution of TNTs from inter-tubular region would be enhanced with further increase in anodizing potential (stage 4 and 5). It has been evaluated that the balance between dissolution and growth reactions would decide the final morphology of the nano-tubular structure and is influenced by the magnitude of applied potential.

4. Conclusion

In this study, the possible reaction mechanism of titanium oxide nano-tubular structure formation has been proposed based on the electrochemical results at potential ($\leq$ 8 V). It has been evaluated from the LSV and PSP analyses that there exists a stable oxide film below a critical potential ($\leq$ 1.9 V) in the F^- containing electrolyte. Beyond this

potential the development of Lewis acid active sites within the oxide film would accelerate the migration of anionic species (F^-, $H_2PO_4^{2-}$ etc.) towards the surface. These species could form the soluble complexes ($[TiF_6]^{2-}$) which resulted in the formation of nano–tubular structure. It has been deduced from the results that the formation of this typical morphology strongly depends on the migration of Ti^{4+} and F^- ions towards the O/E and M/O interface under applied electric field. In the XRD patterns, the shift in peaks at low potential < 1.9 V and increase in their intensity at high potential also confirmed the formation of oxygen deficient Ti_6O phase in the surface film. The competitive growth and localized dissolution of the oxide film would take place beyond a critical potential which is reported as 1.9 V vs. SCE in our case. In support with the LSV and PSP analysis the surface features revealed under SEM and simulated EEC models for the impedance spectra also supported the proposed reaction sequence.

References

[1] K.M. Deen, A. Farooq, M.A. Raza, W. Haider, Effect of electrolyte composition on TiO_2 nanotubular structure formation and its electrochemical evaluation, Electrochim. Acta 117 (2014) 329–335.

[2] K.M. Deen, A. Farooq, M.A. Raza, R. Ahmad, W. Haider, Estimating the degradation of methylethionium chloride dye on nanotubular TiO_2 structure, J. Ind. Eng. Chem. 22 (2015) 153–158.

[3] Z. Rahman, L. Pompa, W. Haider, Influence of electropolishing and magnetoelectropolishing on corrosion and biocompatibility of titanium implants, J. Mater. Eng. Perform. 23 (11) (2014) 3907–3915.

[4] D. Gong, C.A. Grimes, O.K. Varghese, W. Hu, R.S. Singh, Z. Chen, E.C. Dickey, Titanium oxide nanotube arrays prepared by anodic oxidation, J. Mater. Res. 16 (12) (2001) 3331–3334.

[5] K.M. Deen, E. Asselin, Differentiation of the non-faradaic and pseudocapacitive electrochemical response of graphite felt/$CuFeS_2$ composite electrodes, Electrochim. Acta 212 (2016) 979–991.

[6] K. Lee, A. Mazare, P. Schmuki, One-dimensional titanium dioxide nanomaterials: nanotubes, Chem. Rev. 114 (19) (Oct. 2014) 9385–9454.

[7] U.H. Shah, Z. Rahman, K.M. Deen, H. Asgar, I. Shabib, W. Haider, Investigation of the formation mechanism of titanium oxide nanotubes and its electrochemical evaluation, J. Appl. Electrochem. (Jun. 2017) 1–13.

[8] U.H. Shah, K.M. Deen, Z. Rahman, H. Asgar, W. Haider, Peculiar behavior of TiO_2 tubular structure for water reduction in dark and under natural light exposure, Mater. Lett. 198 (2017) 188–191.

[9] S.R. Morrison, Electrochemistry at Semiconductor and Oxidized Metal Electrodes, Springer, 2011.

[10] P. Roy, S. Berger, P. Schmuki, P. Schmuki, TiO_2 nanotubes: synthesis and applications, Angew. Chem. Int. Ed. 50 (2011) 2904–2939.

[11] Y. Tang, J. Tao, Z. Dong, J.T. Oh, Z. Chen, The formation of micrometer-long TiO_2 nanotube arrays by anodization of titanium film on conducting glass substrate, Adv. Nat. Sci. Nanosci. Nanotechnol. 2 (4) (Sep. 2011) 45002.

[12] J.M. Macak, L.V. Taveira, H. Tsuchiya, K. Sirotna, J. Macak, P. Schmuki, Influence of different fluoride containing electrolytes on the formation of self-organized titania nanotubes by Ti anodization, J. Electroceram. 16 (1) (Feb. 2006) 29–34.

[13] J. Pan, D. Thierry, C. Leygraf, Electrochemical impedance spectroscopy study of the passive oxide film on titanium for implant application, Electrochim. Acta 41 (7–8) (May 1996) 1143–1153.